High Light Response of the Thylakoid Proteome in Arabidopsis Wild Type and the Ascorbate-Deficient Mutant *vtc2-2*. A Comparative Proteomics Study[1][W]

Lisa Giacomelli, Andrea Rudella, and Klaas Jan van Wijk*

Department of Plant Biology, Cornell University, Ithaca, New York 14853

The thylakoid proteome of chloroplasts contains multiple proteins involved in antioxidative defense, protein folding, and repair. To understand this functional protein network, we analyzed the quantitative response of the thylakoid-associated proteome of Arabidopsis (*Arabidopsis thaliana*) wild type and the ascorbate-deficient mutant *vtc2-2* after transition to high light (HL; 1,000 μmol photons m^{-2} s^{-1}). The soluble thylakoid proteomes of wild type and *vtc2-2* were compared after 0, 1, 3, and 5 d of HL using two-dimensional gels with three independent experiments, followed by a multivariant statistical analysis and tandem mass spectrometry. After 5 d of HL, both wild-type and *vtc2-2* plants accumulated anthocyanins, increased their total ascorbate content, and lost 10% of photosystem II efficiency, but showed no bleaching. Anthocyanin and total ascorbate concentrations in *vtc2-2* were respectively 34% and 20% of wild type, potentially leading to enhanced oxidative stress in *vtc2-2*. Forty-five protein spots significantly changed as a consequence of genotype, light treatment, or both. Independent confirmation was obtained from western blots. The most significant response was the up-regulation of thylakoid YCF37 likely involved in photosystem I assembly, and specific fibrillins, a flavin reductase-like protein, and an aldolase, each located in thylakoid-associated plastoglobules. Fe-superoxide dismutase was down-regulated in *vtc2-2*, while Cu,Zn-superoxide dismutase was up-regulated. *vtc2-2* also showed a systematic up-regulation of a steroid dehydrogenase-like protein. A number of other stress-related proteins, several thylakoid proteases, and lumenal isomerases did not change, while PsbS increased in wild type upon light stress. These findings are discussed in terms of plastid metabolism and oxidative stress defense, and emphasize that understanding of the chloroplast stress-response network must include the enzymatic role of plastoglobules.

Chloroplasts are frequently exposed to reactive oxygen species (ROS) in the light, due to high redox potentials, excited states of pigments, and generation of free electrons during photosynthetic electron transport in the thylakoid membrane. To prevent and respond to oxidative stress, a multilayered antioxidative defense system is expressed in the chloroplast, which includes enzymatic and nonenzymatic antioxidants (Niyogi, 2000; Mullineaux and Karpinski, 2002; Apel and Hirt, 2004; Mittler et al., 2004; Foyer and Noctor, 2005).

The major antioxidant species in chloroplasts are water soluble ascorbate (vitamin C) and glutathione, as well as lipid soluble carotenoids and α-tocopherol (vitamin E). Ascorbate is a cofactor of thylakoid-bound and stromal ascorbate peroxidases that detoxify hydrogen peroxide (H_2O_2) produced by superoxide dismutases (SODs). Ascorbate in the lumen is the electron donor in the enzymatic conversion of violaxanthin to zeaxanthin by the lumenal violaxanthin deepoxidase. Ascorbate also reduces oxidized vitamin E (Veljovic-Jovanovic et al., 2001; Pastori and Foyer, 2002).

Several ascorbate-deficient mutants were identified in Arabidopsis (*Arabidopsis thaliana*) in a screen for ozone sensitivity (Conklin et al., 2000). Among them, the *vtc2-2* mutant accumulates the lowest levels of ascorbate (10%–20%), is smaller than wild type, and has reduced nonphotochemical quenching (Veljovic-Jovanovic et al., 2001; Müller-Moulé et al., 2002). The mutant has a missense mutation in a predicted exon of At4g26850 with unknown function (Jander et al., 2002). Despite the strongly reduced ascorbate content, *vtc2-2* was able to grow at high light (HL) intensities, but showed oxidative damage upon transition from low to very HL intensities (1,800 μmol photons m^{-2} s^{-1}; Müller-Moulé et al., 2003; Müller-Moulé et al., 2004). The response to ascorbate deficiency (at 200 μmol photons m^{-2} s^{-1}) of another *vtc* mutant (*vtc1*) was analyzed by microarrays (Kiddle et al., 2003; Pastori et al., 2003). Several additional microarray studies were carried out for other mutants and wild type to follow oxidative stress responses (Rossel et al., 2002; Davletova et al., 2005; Mahalingam et al., 2005). The systematic response of the chloroplast proteome to ascorbate deficiency and HL is not known.

The lumenal, peripheral, and integral thylakoid proteomes have been analyzed in significant depth (Gómez et al., 2002; Peltier et al., 2002; Schubert et al., 2002; Friso et al., 2004; Peltier et al., 2004). These

[1] This work was supported by the U.S. Department of Agriculture (Plants and Environment grant no. 0195698 to K.J.v.W.).

* Corresponding author; e-mail kv35@cornell.edu; fax 607–255–3664.

The author responsible for distribution of materials integral to the findings presented in this article in accordance with the policy described in the Instructions for Authors (www.plantphysiol.org) is: Klaas Jan van Wijk (kv35@cornell.edu).

[W] The online version of this article contains Web-only data.

Article, publication date, and citation information can be found at www.plantphysiol.org/cgi/doi/10.1104/pp.106.080150.

systematic proteome analyses, combined with many functional studies, have shown that numerous thylakoid (associated) proteins function in antioxidant defense and/or repair of the thylakoid system (for review, see van Wijk, 2004). These include 2-Cys peroxiredoxin A (2-Cys Prx A), three m-type thioredoxins (Shürmann and Jacquot, 2000; Dietz and Scheibe, 2004; Buchanan and Balmer, 2005), Fe- and Cu,Zn-SODs (Mittler et al., 2004), as well as enzymes and structural proteins involved in biosynthesis and binding of carotenoids and/or quenching of excess light energy (Bassi and Caffarri, 2000; Holt et al., 2004). A family of thylakoid-bound proteins, named fibrillins (FIBs), was shown to play a role in stress response, including oxidative stress (Gillet et al., 1998; Monte et al., 1999; Rey et al., 2000; Langenkämper et al., 2001). These FIBs are not enzymatically active but form a protein coat of lipid-rich particles named plastoglobules (PGs) that are associated to thylakoids (Kessler et al., 1999; Vidi et al., 2006; Ytterberg et al., 2006). These PGs also contain various quinones and α-tocopherol, as well as a significant set of proteins likely involved in metabolism of isoprenoid-derived molecules (quinones and tocopherol), lipids, and carotenoid cleavage. Thus, PGs are likely to play a role in various metabolic pathways and oxidative stress defense (Vidi et al., 2006; Ytterberg et al., 2006).

In this work, we analyzed a time course of the Arabidopsis thylakoid lumenal, peripheral, and PG proteome of wild type and *vtc2-2* after the transition from optimal light conditions (approximately 120 μmol photons m^{-2} s^{-1}) to HL (1,000 μmol photons m^{-2} s^{-1}). We used denaturing two-dimensional gel electrophoresis (2DE) followed by image analysis. The experiment comprised three technical replicates, three independent experiments, and a multivariant statistical analysis. Fourty-five protein spots significantly changed ($P < 0.05$) as a consequence of the genotype, the light treatment, and/or their interaction. Proteins were identified by tandem mass spectrometry (MS) and independent expression analysis was obtained by western-blot analysis for selected proteins. These findings are discussed in terms of plastid metabolism and oxidative stress defense.

RESULTS

Phenotypic Response of Wild Type and *vtc2-2* to the HL Treatment; Setting the Stage for Proteome Analysis

Wild-type and *vtc2-2* plants were grown on soil under a short-day length at optimal light intensity (120 μmol photons m^{-2} s^{-1}) for about 40 d to reach a fully developed rosette. Throughout the remainder of this article, we refer to the *vtc2-2* line as *vtc2*. As expected, *vtc2* plants were reduced in size and biomass as compared to wild type (Fig. 1A). Light intensity was then increased to 1,000 μmol photons m^{-2} s^{-1} under otherwise identical conditions. Surprisingly, after 3 and 5 d of HL, *vtc2* visibly accumulated less anthocyanins than wild type, in particular when viewing the adaxial side of the leaves (Fig. 1B). After 5 d of HL, wild type rosettes accumulated about 176 μg total monomeric anthocyanin per gram fresh weight, whereas *vtc2* accumulated only 61 μg per gram fresh weight corresponding to 34% of wild-type levels (Fig. 2A).

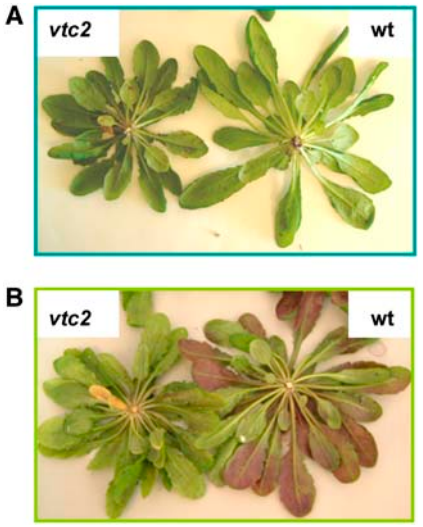

Figure 1. Photos of fully grown wild-type and *vtc2* rosettes (showing the adaxial sides) before (A) and after 5 d of HL treatment (B). HL-induced anthocyanin accumulation is visible in wild type but not in *vtc2*.

Total oxidized and reduced ascorbate concentrations in *vtc2* leaves were about 20% of wild-type levels under the optimal light conditions. Total ascorbate concentrations nearly doubled after 5 d of HL in both genotypes (Fig. 2B). About 5% to 8% of the total ascorbate was oxidized in wild type under both light conditions, while 27% to 33% of total ascorbate was oxidized in *vtc2* under both light conditions. Thus, the already smaller pool of ascorbate in *vtc2* appeared more oxidized; we note that it is possible that this oxidation is somewhat overestimated due to some interference by oxidation of dithiothreitol used in the assay (Takahama and Oniki, 1992).

To monitor the efficiency of PSII, one of the prime targets for light-induced damage, we measured the chlorophyll fluorescence maximum photochemical efficiency of PSII in the dark-adapted state (F_v/F_m) ratio of dark-adapted leaves about 2 h into the light period. F_v/F_m ratios were 0.84 for both wild type and *vtc2* prior to the HL treatment and decreased to about 0.75 and 0.72 after 5 d of HL in wild type and *vtc2*, respectively (Fig. 2C). These measurements showed that the HL-induced loss of PSII efficiency ranged from 11% to 14%, with no significant differences between wild type and *vtc2*.

Outline of the Thylakoid Proteome Analysis by 2DE Analysis

The phenotypic analysis above clearly showed a moderate light-induced oxidative stress (reduced

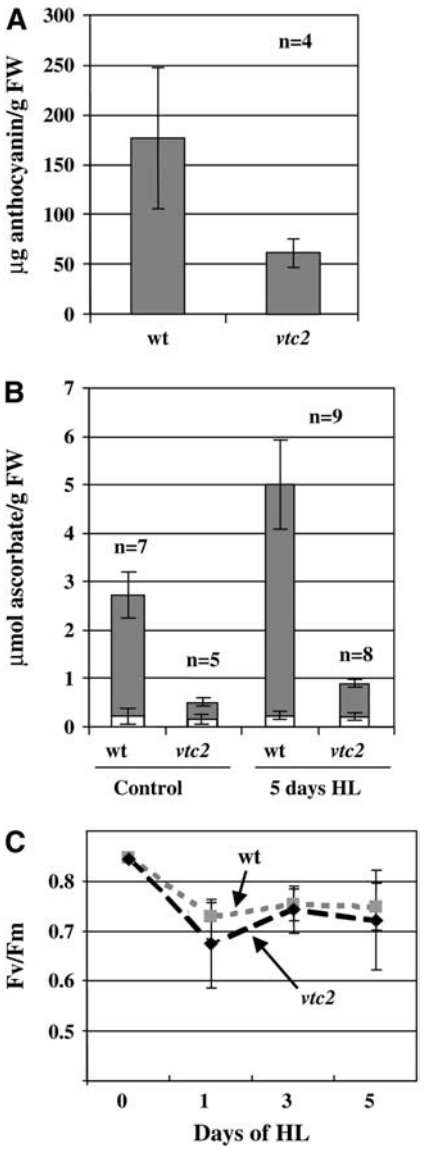

Figure 2. Quantified response of several physiological leaf parameters of wild type and *vtc2* before and after 5 d of HL treatment. A, Anthocyanin accumulation of wild-type and *vtc2* rosettes after 5 d of HL ($n = 4$). B, Accumulation of total ascorbate (ascorbate + dehydro ascorbate) as the sum of oxidized (white bars) and reduced ascorbate (gray bars) in wild type and *vtc2* before or after 5 d of HL. C, Chlorophyll fluorescence F_v/F_m ratio of wild-type and *vtc2* dark-adapted leaves before and after 1, 3, and 5 d of HL. SD is indicated ($n = 10$–21).

F_v/F_m, doubling of ascorbate, and accumulation of anthocyanins) in both wild type and *vtc2*. To analyze the HL response of the peripheral, lumenal, and PG thylakoid proteomes in *vtc2* and wild type, thylakoids were purified prior to the HL treatment (0 d) and after 1, 3, and 5 d of HL. After thylakoid purification, the peripheral and lumenal thylakoid and PG proteomes were extracted by sonication and analyzed by 2DE, using immobilized pH gradient (IPG) strips in the first dimension (pI 4–7) and gradient SDS-PAGE (8%–16% acrylamide) in the second dimension.

To allow statistical analysis of the differential expression of this extracted thylakoid proteome in response to light and ascorbate deficiency, the complete experiment was repeated three times, including plant growth, proteome purification, and 2DE. Throughout this manuscript, these three independent experiments are named biological replicates. To reduce gel-to-gel variation, each protein preparation was analyzed on at least three parallel 2DE gels. In total we generated and analyzed 72 2DE gels (two genotypes, three gel replicates, four time points, and three biological replicates).

2DE Analysis of the Lumenal and Peripheral Thylakoid and Plastoglobular Proteome

The gel images looked overall quite similar to each other, both when comparing wild type and *vtc2* and when comparing different time points (Fig. 3, A and B). This indicated that the thylakoid purifications, protein extractions, 2DE, and gel staining were reproducible. Spots were first automatically (using image analysis software) detected in all 72 gel images using the same parameters for all gels (e.g. sensitivity and background). Subsequently, a manual spot editing was carried out for each of the gel images to remove minor features resulting from, for example, Sypro Ruby precipitates, and to split major trains of spots into single spots. All spots were then quantified and normalized to their respective total gel spot volume. After this first-pass manual curation, gel images were matched to a reference gel (Supplemental Fig. 1). Spots not present on the reference gel were added if they were present on at least five gels; in total, 328 spots were assigned on this reference gel. Intensities of corresponding spots on the three technical gel replicates within a genotype-treatment combination were averaged. A total of 155 out of 328 spots had an averaged intensity for all 24 combinations (genotype-treatment-biological replicates) and are hereafter assigned as the complete data set (Supplemental Table I). This set was used for statistical analysis.

Statistical Analysis and Protein Identification by Tandem MS

We tested the effect of the HL treatment and the genotype, as well as their interaction, on the complete data set using a multivariance analysis. At $P < 0.01$, we observed a significant genotype effect and significant treatment effect for 10 spots each and a significant genotype-treatment interaction (this means that the difference between the two genotypes changes significantly upon the treatment) for two spots, totaling 20 spots (Fig. 4). When the P value was increased to $P < 0.05$, 45 significant spots were detected (Fig. 4). All significant spots were analyzed by nano liquid chromatography electrospray tandem mass spectrometry (ESI-MS/MS) and proteins could be identified in most spots. A number of spots contained more than one protein, and for some of them it was not possible to

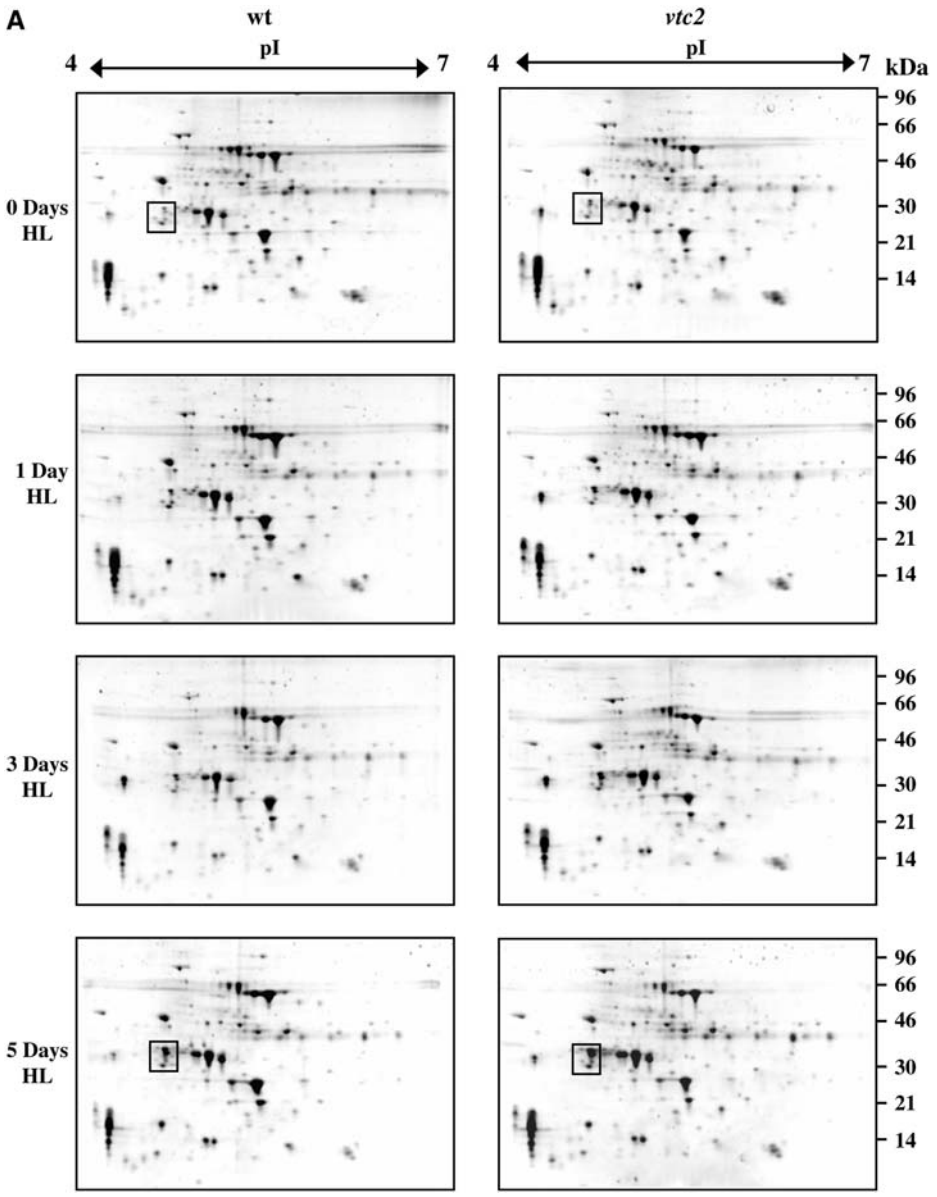

Figure 3. Sypro Ruby-stained 2DE gels of the peripheral and lumenal thylakoid proteome of wild type and *vtc2*. A, Representative gels prior to HL treatment and after 1, 3, or 5 d of HL. Close ups of the framed areas are shown in B. B, Close up of the area with spots 263 and 271, containing several FIBs, at 0 and 5 d of HL. Three representative gels for wild type and *vtc2* are shown for each time point.

determine which one was the main component (data not shown). We will not discuss spots in which no proteins were identified nor spots that contained a mixture of proteins of quite equal abundance. In total, 19 spots and their protein identities will be discussed and are listed in Table I, together with a graphic display of the averaged relative spot intensities with SD for each genotype-treatment combination. A reference gel with these 19 significant protein spots is shown in Supplemental Figure 1 (spot numbers in blue).

Light Treatment Effect

Most of the spots that significantly responded to the light treatment were increasingly up-regulated with progressive days of light stress (spot nos. 149, 202, 261, 263, 271, 284, 421, 851, and 1,010; Table I). Spot 149 contained FIB2 (At2g35490) and spots 261, 263, 271, and 284 all contained FIB1a,1b (At4g04020 and At4g22240). Spots 261 and 271 also contained low levels of FIB4 (At3g23400) and FIB7a (At3g58010), respectively. These proteins are all members of the FIB family (Table I). A close up of the 2DE spots 263 and 271 is shown in Figure 3B. Spot 202 contained Fru biphosphate aldolase-1 (At2g21330) that was recently shown to accumulate in PGs, in addition to its abundant accumulation in the chloroplast stroma (Vidi et al., 2006; Ytterberg et al., 2006). Spot 421 contained a homolog to YCF37 in Synechocystis (At2g23670) and increased 2-fold over 5 d of light treatment. Spot 1,010 contained a flavin reductase-related protein (At1g32220) with background signals of Ser-type protease subunit ClpP4 (At5g45390) and an RNA-binding protein (CP29B′; At2g37220). CP29B′ was a minor contamination of an abundant neighboring spot.

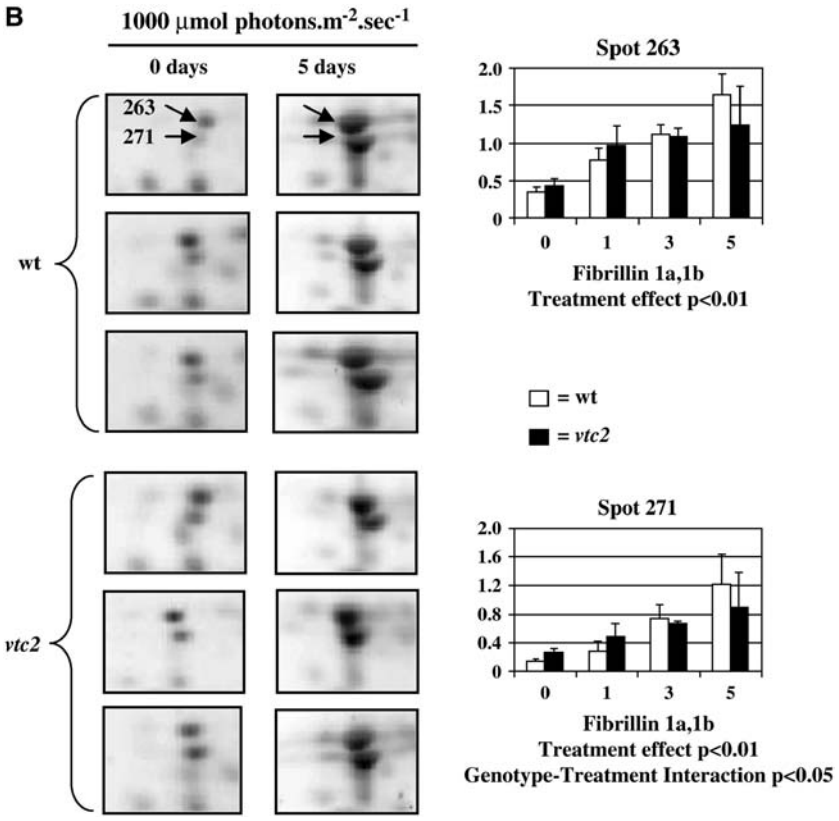

Figure 3. (*Continued.*)

In contrast to the up-regulation in the spots above, spot 262, containing a putative glyoxylase (lactoylglutathione lyase; At1g67280), was down-regulated 3-fold in wild type but not significantly effected in *vtc2.* Spot 851 contained the chaperones cpHSP70-1,2 (At4g24280 and At5g49910) and showed an increase in *vtc2* after 3 and 5 d of HL, but no change in accumulation in the wild type. Spot 324 contained an OEC23-like protein and showed a small, but consistent increase in *vtc2*. Spot 351 was weak, containing a breakdown product of 2-Cys Prx A and increased slightly after 3 and 5 d HL. However, for spot 157 (see sections below) containing the mature 2-Cys Prx A, no significant change was observed; this was confirmed by western blotting (data not shown). Spot 377 also contained an OEC23-like protein (but different from spot 324) and was down-regulated upon light treatment. Spot 390 contained Cu,Zn SOD that was consistently more abundant in *vtc2*.

Genotype Effect

Seven identified spots (262, 289, 314, 324, 390, 427, and 851) showed a significant ($P < 0.01$ or $P < 0.05$) differential response to the genotype (wild type versus *vtc2*). Spot 289 contained a mix of 3-β-hydroxy-δ-steroid dehydrogenase (At2g37660) and the OEC33-like protein (At3g50820) with consistent up-regulation in *vtc2*. As mentioned above, spot 390 contained Cu,Zn-SOD and was consistently more abundant in *vtc2*. Spot 427 contained a breakdown product of one of the two plastocyanin homologs, PC-2 (At1g76100), and was also higher in *vtc2*. The response to the genotype of spots 262 and 851 was also significantly different for the HL treatment (at $P < 0.05$ and 0.01, respectively). As mentioned in the previous paragraph, spot 262 containing a glyoxylase I (also named lactoylglluthathione lyase) was down-regulated in wild type but not significantly affected in *vtc2*. Spot 851 contained the chaperones cpHSP70-1,2 (At4g24280 and At5g49910) and showed an increase in *vtc2* in response to 3 and 5 d of HL but no change in accumulation in the wild type. Neighboring spot 314 contained Rib 5-P isomerase (At3g04790) and was consistently higher in *vtc2* than in wild type.

Spots with Only Significant Plant-Treatment Interaction

Two spots (285 and 964) showed only a significant ($P < 0.05$) genotype-treatment interaction and no effect of genotype or treatment alone. Spot 285 contained FIB1a (At4g22240) and FIB7a (At3g58010). The spot showed a higher accumulation at time point 0 in *vtc2*, but a higher accumulation at time point 5 d of HL in wild type. Spot 964 contained cpHSP70-2 and its closely related homolog cpHSP70-1 with lower MOWSE score. This spot is located close to spot 851 also containing these two HSP70 homologs, as discussed in the

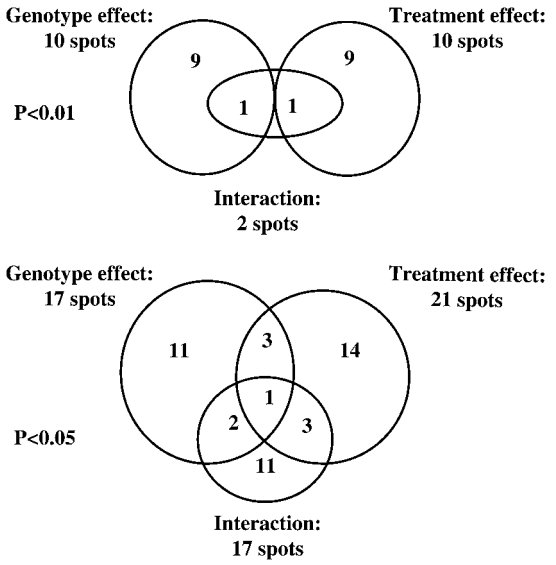

Figure 4. Venn diagrams of spots showing significant differences ($P < 0.01$ or $P < 0.05$) between wild type and *vtc2* (genotype effect), between control and HL treatment, and/or showing a differential response to the HL treatment independent of the genotypes. The complete data set is available as Supplemental Table I.

previous section. Spot 964 showed a small increase in cpHSP70 levels in *vtc2* as compared to wild type at the later time points, consistent with the observations for spot 851.

Independent Confirmation of 2DE Results

We confirmed the up-regulation of FIBs observed by 2DE using SDS-PAGE and western blots on total membrane protein extracts (Fig. 5A). Prior to light stress, the FIBs could hardly be observed, but their intensity increased several fold after 1 and 3 d of light stress in both wild type and *vtc2*, with a slightly stronger response in *vtc2* than in wild type, in agreement with the 2DE analysis. As also observed by 2DE, FIB accumulation did not increase from 3 to 5 d in *vtc2*, but did increase in this interval in wild type. To ensure that the observed increase was not related to binding and release of FIBs to the membrane, we also blotted the total soluble fraction (Fig. 5A). As expected, only a weak signal from FIB1a was observed. This is in agreement with our proteome analyses of chloroplast subfractions showing that FIBs typically associate with thylakoids.

We confirmed the up-regulation of Cu,Zn-SOD in *vtc2* as compared to wild type (spot 390) using one-dimensional gels and western blots on total soluble extracts (Fig. 5B). At each time point we observed an up-regulation of Cu,Zn-SOD in *vtc2* as compared to wild type. Since expression of Cu,Zn-SOD is antagonistic to expression of the three chloroplast-localized Fe-SODs in the chloroplast under copper deficiency (Abdel-Ghany et al., 2005), we also determined total Fe-SOD accumulation levels in total soluble extracts (Fig. 5B). Indeed, the Fe-SODs were down-regulated in *vtc2* as compared to wild type.

Proteins That Do Not Significantly Change in Response to the Transition to HL or Genotype

In addition to the statistical analysis and identification of differentially expressed proteins, we also specifically looked at the accumulation patterns of known lumenal and peripheral thylakoid proteins that are associated with oxidative stress defense, redox regulation, proteolysis, and (un) folding. To facilitate this analysis, we identified the proteins in most of the spots on the 2DE gels by MS/MS. In total, 99 proteins were identified, of which 91% were chloroplast predicted by TargetP (see Supplemental Table II). This set included eight proteases, eight chaperones and isomerases, 13 stress-related proteins, eight RNA-binding and ribosomal proteins, 14 proteins of the photosynthetic apparatus, and many proteins without known function or with diverse functions in metabolism (Supplemental Table II). We extracted the spot quantifications and statistical analysis for the most relevant 13 spots in which only one protein (or one dominant protein) was identified. Details for those spots are listed in Table II (13 spots) and they are also marked (in black) on the reference gel (Supplemental Fig. 1). Examples were proteases DegP5 (spot 251), DegP8 (spot 181), DegP1 (abundant spots 957 and 203), and thioredoxin type m1 (major component in spots 424 and 428 and uniquely in spot 976). Also, the stromal 2-Cys Prx A in spot 157 did not change. Spot 381 contained peroxiredoxin II E, probably as a major component of the spot, and was not significantly changing either. We do point out however, that even though not significant at $P < 0.05$, some of these spots show a drop after 1 d of HL, followed by an increase in the following days (e.g. spots 424 and 381).

Integral Thylakoid Membrane Proteins Associated with Light Stress

Several integral thylakoid proteins have been associated with oxidative stress. We tested the accumulation of PsbS and thylakoid proteases and FtsH2 (also named VAR2), using western-blot analysis of total membrane proteins of leaves (Fig. 6). PsbS levels doubled during the HL treatment in wild type, without a significant increase in *vtc2* (Fig. 6A). In contrast, FtsH2 level did not change significantly upon light stress and no differences were found between *vtc2* and wild type (Fig. 6B).

DISCUSSION

Collective evidence from various studies has shown that the thylakoid proteome of chloroplasts contains multiple proteins involved in antioxidative defense, protein folding, and repair. Moreover, proteomics studies have shown that the thylakoids contain a

Table I. *Selected differentially accumulating protein spots and details of spot quantification, protein content, and MS-based identification*

The bar diagrams show the average of the spot intensities across the three independent experiments for wild type (white bars) and *vtc2* (black bars) at 0, 1, 3, and 5 d of HL with SDs. Statistical significance as determined by the multivariant analysis is indicated as: G, genotype effect; T, treatment effect; and I, genotype-treatment interaction, with indicated maximum *P* value. Experimental pI and molecular mass (MW) are listed. Protein(s) identified in the spots are listed with the Mascot MOWSE score (or scores if two matched spots were analyzed by MS successfully) as a measure of confidence for MS-based identification. The curated location for each protein is indicated. Asterisks (*) indicate modification from original MapMan Bin.

□ = *wt* ■ = *vtc2*	Effect (*P* <)	Spot No.	Exp. pI	Exp. MW	Accession No.	Protein Name	MapMan Bin	MOWSE Score	Localization
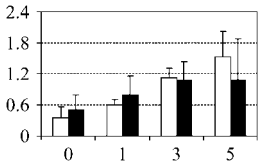	T (0.05)	149	4.3	40	At2g35490	FIB2	26.31* misc. FIBs	320/400	PGs
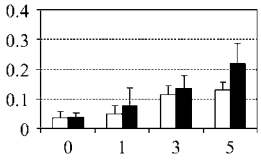	T (0.01)	202	5.2	33	At2g21330	Fructose-bisphosphate aldolase-1	1.3.6 PS.calvin cyle.aldolase; 4.07 glycolysis.aldolase	215	PGs; stroma
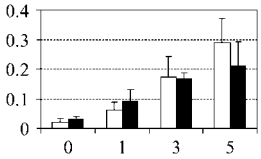	T (0.01)	261	4.6	27	At4g04020	FIB1a	26.31* misc. FIBs	461/619	PGs
					At4g22240	FIB1b	26.31* misc. FIBs	365	PGs
					At3g23400	FIB4	26.31* misc. FIBs	62	PGs
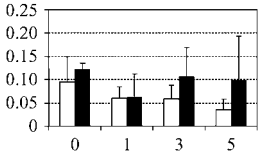	T (0.05), G(0.05), and I (0.05)	262	5.3	27	At1g67280	Glyoxalase I -1 (lactoylglutathione lyase)	13.2.3.2 amino acid metabolism. degradation.aspartate family.threonine; 24 biodegradation of xenobiotics	142/75	Stroma; peripheral thylakoid
					At3g23400	FIB4	26.31* misc. FIBs	56	PGs
					At3g50820	psbO OEC33 like	1.1.1.2 PS.lightreaction. photosystem II.PSII polypeptide subunits	109	Thylakoid lumen
					At5g66570	psbO OEC33	1.1.1.2 PS.lightreaction. photosystem II.PSII polypeptide subunits	109	Thylakoid lumen
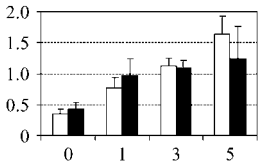	T (0.01)	263	4.7	27	At4g04020	FIB1a	26.31* misc. FIBs	1,224/529	PGs
					At4g22240	FIB1b	26.31* misc. FIBs	703	PGs
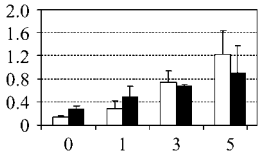	T (0.01) and I (0.05)	271	4.7	26	At4g22240	FIB1b	26.31* misc. FIBs	831/177	PGs
					At4g04020	FIB1a	26.31* misc. FIBs	820	PGs
					At3g58010	FIB7a	26.31* misc. FIBs	151	PGs

(*Table continues on following page.*)

Table I. (*Continued from previous page.*)

□ = *wt* ■ = *vtc2*	Effect ($P <$)	Spot No.	Exp. pI	Exp. MW	Accession No.	Protein Name	MapMan Bin	MOWSE Score	Localization
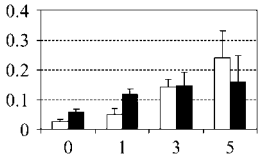	T (0.01) and I (0.01)	284	4.6	26	At4g04020	FIB1a	26.31* misc. FIBs	103/360	PGs
					At4g22240	FIB1b	26.31* misc. FIBs	221	PGs
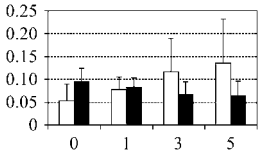	I (0.05)	285	4.7	26	At3g58010	FIB7a	26.31* misc. FIBs	234/148/120	PGs
					At4g22240	FIB1b	26.31* misc. FIBs	165	PGs
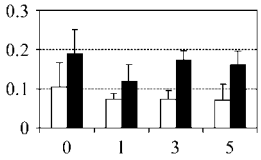	G (0.01)	289	5.2	24	At2g37660	3-β-Hydroxy-δ5-steroid dehydrogenase	35.2 not assigned. unknown	257	Stroma; peripheral thylakoid
					At3g50820	psbO OEC33 like	1.1.1.2 PS.lightreaction. photosystem II.PSII polypeptide subunits	206	Thylakoid lumen
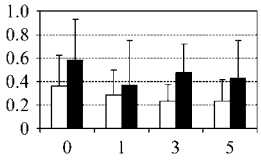	G (0.01)	314	4.9	23	At3g04790	Ribose 5-phosphate isomerase	1.3.10 PS.calvin cyle.Rib5P isomerase; 7.2 OPP. nonreductive PP	397/341	Stroma; peripheral thylakoid
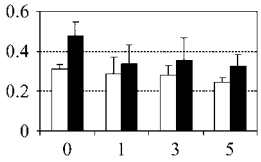	T (0.05) and G (0.05)	324	6.0	26	At4g15510	OEC23-like-3 Tat lTP	1.1.1.2 PS.lightreaction. photosystem II.PSII polypeptide subunits	101/450	Thylakoid-peripheral-lumenal side
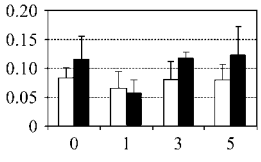	T (0.05)	351	4.8	20	At3g11630	2-Cys Prx A	21.5 redox.periredoxins	45	Stroma; peripheral thylakoid
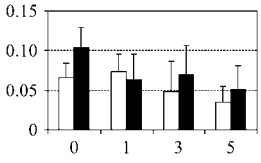	T (0.05)	377	5.4	17	At2g28605	PsbP domain-OEC23 like	1.1.1.2 PS.lightreaction. photosystem II.PSII polypeptide subunits	44/291	Thylakoid-peripheral-lumenal side
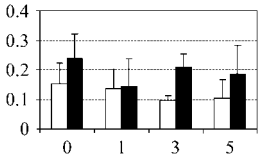	G (0.01)	390	5.4	16	At2g28190	Cu,Zn-SOD (CSD2)	21.6 redox.dismutases and catalases	262/86/60	Stroma; peripheral thylakoid

(*Table continues on following page.*)

Table I. (*Continued from previous page.*)

□ = *wt* ■ = *vtc2*	Effect ($P <$)	Spot No.	Exp. pI	Exp. MW	Accession No.	Protein Name	MapMan Bin	MOWSE Score	Localization
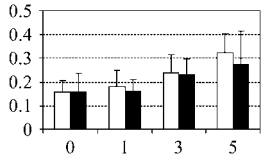	T (0.01)	421	4.6	14	At2g23670	ycf37 Synechocystis	35.2 not assigned.unknown	65/151	Thylakoid
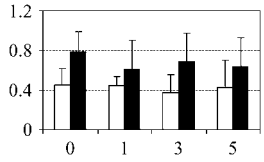	G (0.01)	427	4.5	14	At1g76100	PC-2 fragment	1.1.5.1 PS.lightreaction. other electron carrier (ox/red).plastocyanin	42/56	Thylakoid-peripheral-lumenal side
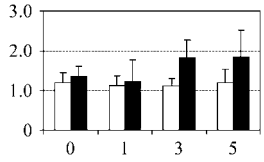	G (0.01) and I (0.01)	851	4.8	69	At4g24280	cpHSP70-1	29.6* protein.(un)folding (includes isomerases and chaperones, if not heat induced)	895/513	Stroma; peripheral thylakoid
					At5g49910	cpHSP70-2	29.6* protein.(un)folding (includes isomerases and chaperones, if not heat induced)	354	Stroma; peripheral thylakoid
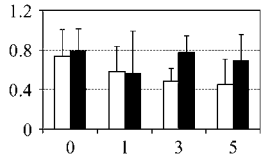	I (0.05)	964	4.9	69	At5g49910	cpHSP70-2	29.6* protein.(un)folding (includes isomerases and chaperones, if not heat induced)	691/381	Stroma; peripheral thylakoid
					At4g24280	cpHSP70-1	29.6* protein.(un)folding (includes isomerases and chaperones, if not heat induced)	239	Stroma; peripheral thylakoid
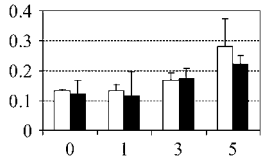	T (0.01)	1,010	4.7	24	At1g32220	Flavin reductase-related (3β_HSD; Isoflavone_redu)	35.2 not assigned.unknown	65/247	PGs
					At2g37220	RNA-binding protein CP29 B′	27.4 RNA.RNA binding	138	Stroma; peripheral thylakoid
					At5g45390	ClpP4	29.5.5 protein.degradation. serine protease	72	Stroma; peripheral thylakoid

significant number of additional proteins, many without known function. However, it is not clear if and how these individual proteins are coregulated in response to HL stress and how reduced cellular ascorbate content possibly alters this response. To fill this void, the primary objective of this study was to determine the collective response of the lumenal- and thylakoid-associated proteins following a transition from 120 μmol photons m^{-2} s^{-1} to HL (1,000 μmol photons m^{-2} s^{-1}). We included the ascorbate-deficient mutant *vtc2* to enhance the oxidative stress levels and alter the oxidative stress network and to look for specific stress resulting from ascorbate deficiency. We postulated that since the antioxidative defense system has several overlapping strategies, weakening one of the ROS detoxification mechanisms would allow better detection of the functional network and functional relationships between different protein components.

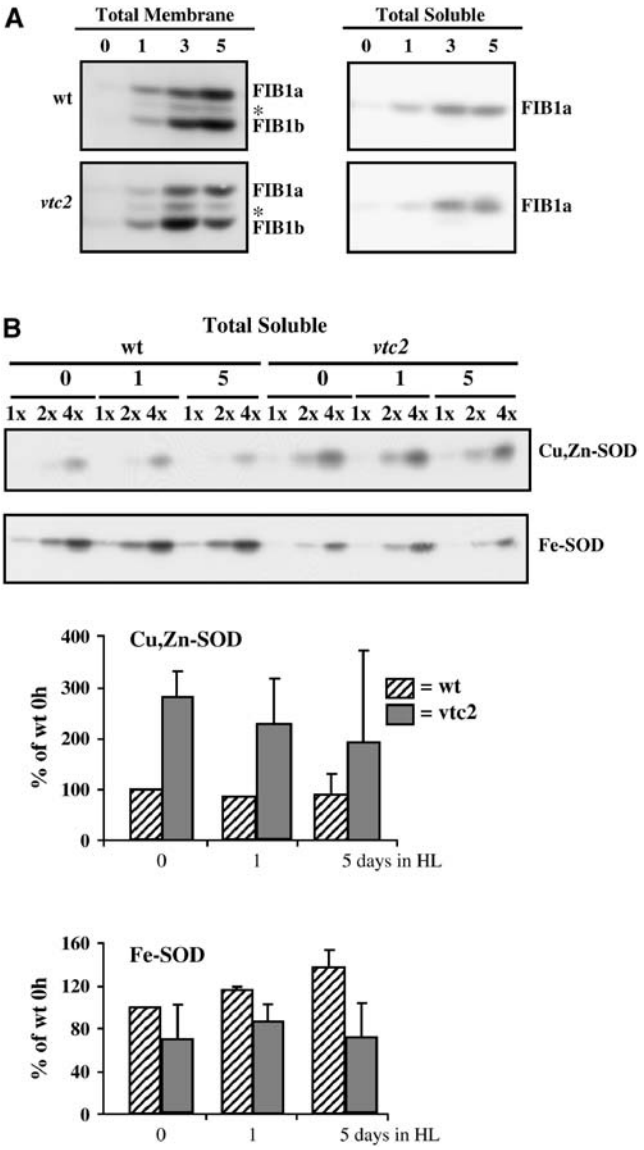

Figure 5. Western-blot analysis of the chloroplast response to the HL treatment. A, Western-blot analysis with anti-FIB antibody of total membrane proteins and soluble proteins from leaves of wild type and *vtc2*. One-hundred micrograms of proteins were loaded per gel lane. The identity of the cross-reacting bands (FIB1a,b) was confirmed by parallel 2-DE gels of extracted thylakoid proteins. The weak band (marked with an asterisk) between FIB1a and FIB1b is likely FIB4. B, Western-blot analysis with anti-chloroplast Cu,Zn-SOD and with anti-chloroplast Fe-SOD of total soluble leaf extract of wild type and *vtc2* after 0, 1, and 5 d of HL treatment. A total of 10, 20, and 40 μg of proteins were loaded per gel lane (indicated as 1x, 2x, and 4x). The experiment was repeated twice with independent biological replicates ($n = 2$). The bar diagrams show the quantification for both Cu,Zn-SOD and Fe-SOD with SDS.

The Physiological Response to HL and the Consequence of Ascorbate Deficiency

The physiological response of *vtc2* plants to a transition from low light (150–180 μmol photons m^{-2} s^{-1}) to very HL levels (1,500–1,800 μmol photons m^{-2} s^{-1}) was analyzed in two recent studies (Müller-Moulé et al., 2002; Müller-Moulé et al., 2003). Short-term (up to 2 h) HL exposure did not lead to significant loss of PSII efficiency (as measured by F_v/F_m), but *vtc2* leaves showed a reduced conversion rate of violaxanthin to zeaxanthin, due to the ascorbate dependency of violaxanthin deepoxidase located in the thylakoid lumen (Müller-Moulé et al., 2002). In a subsequent study with more long-term exposure of *vtc2* to very HL (up to 5 d at 1,800 μmol photons m^{-2} s^{-1}), the authors showed that older leaves bleached with increased degree of damage to PSII and lipid peroxidation, ultimately leading to necrosis (Müller-Moulé et al., 2003). It is a valid question whether the total ascorbate concentration in the leaf represents the ascorbate concentration in the chloroplast. This point was partially answered in (Müller-Moulé et al., 2002) by showing that the ascorbate availability in *vtc2* did limit violaxanthin deepoxidase activity in the thylakoid lumen in vivo. This demonstrates that ascorbate concentration in chloroplasts of *vtc2* leaves is lower than in wild type.

In this study, prior to the planned proteome analysis, we defined and compared the physiological states of wild type and *vtc2* during HL treatment to ensure that the extensive proteome analysis would be meaningful. Importantly, we wanted to avoid light-induced leaf bleaching and necrosis since these are very dramatic and pleiotropic responses, leading to complete loss of chloroplasts and cell integrity. We aimed at finding a condition that resulted in a minor light-induced decrease of photosynthetic electron transport and that avoided bleaching. Using 1,000 μE m^{-2} s^{-1}, light-induced loss of PSII efficiency was less than 10% for wild type and *vtc2*, whereas cellular ascorbate concentration doubled both in wild type and *vtc2*. Interestingly, ascorbate levels in *vtc2* remained at approximately 20% of wild type at each of the time points (0, 1, 3, and 5 d of HL). Ascorbate appeared more oxidized in *vtc2* than in wild type, but some of that could be due to interference by low levels of oxidized dithiothreitol.

Surprisingly, during the HL treatment, wild-type plants but not *vtc2* turned red from accumulation of anthocyanins that were 3-fold lower in *vtc2* than in wild type. Anthocyanins accumulate upon various stresses and have been reported to be ROS scavengers (Nagata et al., 2003). A recent microarray analysis of Arabidopsis plants exposed to HL identified a transcriptional cluster with the complete known anthocyanin regulatory and biosynthetic pathway that was strongly and rapidly induced by HL in control plants (Vanderauwera et al., 2005). Increased levels of cellular H_2O_2 (by a combination of catalase deficiency and HL) led to repression of this gene cluster (Vanderauwera et al., 2005). It is also known that (reduced) ascorbate is required in the anthocyanin biosynthetic pathway (Wilmouth et al., 2002). Possibly, higher concentrations of H_2O_2 lead to oxidation of ascorbate. Thus, the repression of anthocyanin accumulation in *vtc2* as compared to wild type likely resulted from the restricted availability of reduced ascorbate.

Table II. *Quantification of proteins involved in stress response and/or protein biogenesis and degradation in quantified and reproducible spots that do not show a significant response (at $P < 0.05$) to the HL treatment, the genotype, or the interaction*

Details of spot quantification, protein content, and MS-based identification are listed. The bar diagrams show the average of the spot intensities across the three independent experiments for wild type (white bars) and *vtc2* (black bars) at 0, 1, 3, and 5 d of HL with SDS. Protein(s) identified in the spots are listed with the Mascot MOWSE score as a measure of confidence for MS-based identification. The curated location for each protein is indicated. Asterisks (*) indicate modification from original MapMan Bin.

Quantification □ = *wt* ■ = *vtc2*	Spot No.	Exp. pI	Exp. MW	Accession No.	Protein Name	MapMan Bin	MOWSE Score	Localization
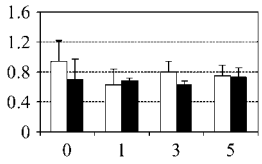	187	5.2	34	At4g17740	CtpA-1	29.9* protein. processing	152	Thylakoid-peripheral-lumenal side
				At1g32060	Phosphoribulokinase-2	1.3.12 PS. calvin cyle.PRK	51	Stroma
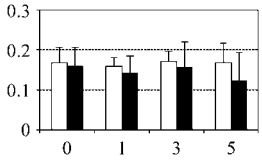	251	4.9	28	At4g18370	DegP5	29.5 protein. degradation	428	Thylakoid-peripheral-lumenal side
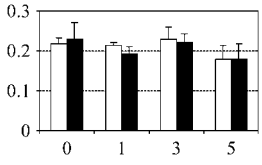	181	6.1	36	At5g39830	DegP8	29.5.5 protein. degradation. serine protease	339	Thylakoid-peripheral-lumenal side
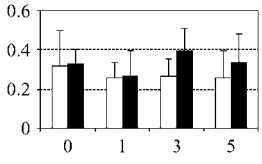	82	4.9	57	At2g28000	Cpn60-α-1	29.6* protein.(un)folding (includes isomerases and chaperones, if not heat induced)	757	Stroma
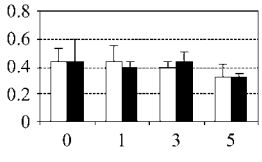	373	5.3	17	At2g43560	FKBP-type peptidyl-prolyl cis-trans isomerase	29.6* protein.(un)folding (includes isomerases and chaperones, if not heat induced)	212	Thylakoid-peripheral-lumenal side
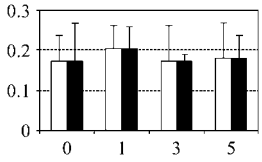	177	5.1	36	At3g15520	Peptidyl-prolyl cis-trans isomerase TLP38	29.6* protein.(un)folding (includes isomerases and chaperones, if not heat induced)	580	Thylakoid-peripheral-lumenal side
				At2g21330	Fructose-bisphosphate aldolase-1	1.3.6 PS.calvin cyle. aldolase; 4.07 glycolysis.aldolase	54	Stroma (1); plastoglobules (2)
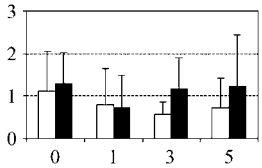	368	5.5	17	At3g62030	Peptidylprolyl isomerase ROC4	29.6* protein.(un)folding (includes isomerases and chaperones, if not heat induced)	60/391	Stroma

(*Table continues on following page.*)

Table II. (*Continued from previous page.*)

Quantification □ = *wt* ■ = *vtc2*	Spot No.	Exp. pI	Exp. MW	Accession No.	Protein Name	MapMan Bin	MOWSE Score	Localization
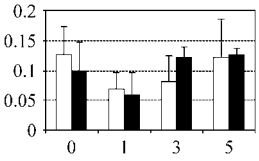	424	4.6	14	At1g03680	Thioredoxin m1	21.1 redox. thioredoxin	260	Thylakoid-peripheral-stromal side
				At2g23670	Ycf37 Synechocystis	35.2 not assigned. unknown	60	Thylakoid
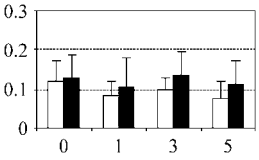	157	4.9	39	At3g11630	2-Cys Prx A	21.5 redox.periredoxins	363	Thylakoid-peripheral-stromal side
				At5g30510	30S ribosomal protein S1	29.2.1 protein.synthesis. chloroplast-plastid ribosomal protein	50	Stroma
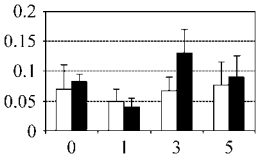	381	4.9	16	At3g52960	Peroxiredoxin II E (PrxE)	21.5 redox.periredoxins	561	Thylakoid-peripheral-stromal side
				At1g76450	OEC23-like-2 Tat lTP	1.1.1.2 PS.lightreaction. photosystem II.PSII polypeptide subunits	142	Thylakoid-peripheral-lumenal side
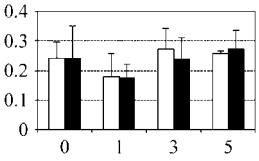	218	5.6	31	At1g20020	FNR-2	1.1.5.3 PS.lightreaction. other electron carrier (ox/red).ferredoxin reductase	162	Thylakoid-peripheral-stromal side
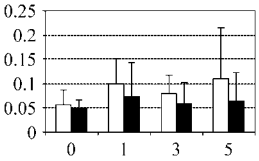	288	4.3	25	At5g07020	Proline-rich protein family	35.1.42 not assigned.no ontology.proline rich family	61/98	Thylakoid
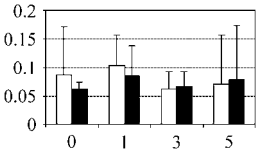	253	5.5	27	At5g54770	THI1 involved in thiamine synthesis (vitamin B; ARA6)	18 cofactor and vitamin E metabolism	127	Plastid (1); mitochondria (2)

Comparative Proteome Analysis

Denaturing 2DE gels have in particular been successful to visualize and identify soluble subfractions of plant (and non plant) proteomes of relative low complexity, such as the mitochondrial matrix, vacuolar, and the soluble thylakoid proteomes. 2DE is also popular for comparative proteomics, but often suffers from problems with reproducibility and lack of (tests of) statistical significance. In this study, considerable efforts were made to obtain statistically significant results in several ways: 1) Each sample was run at least three times on a 2DE gel, 2) first dimensions and second dimensions were run in parallel in batches of 10 to 12 strips/gels, using precast IPG strips and precast gradient gels, 3) gels were loaded with relatively small amounts of proteins (100 μg), 4) the complete experiment was carried out with three

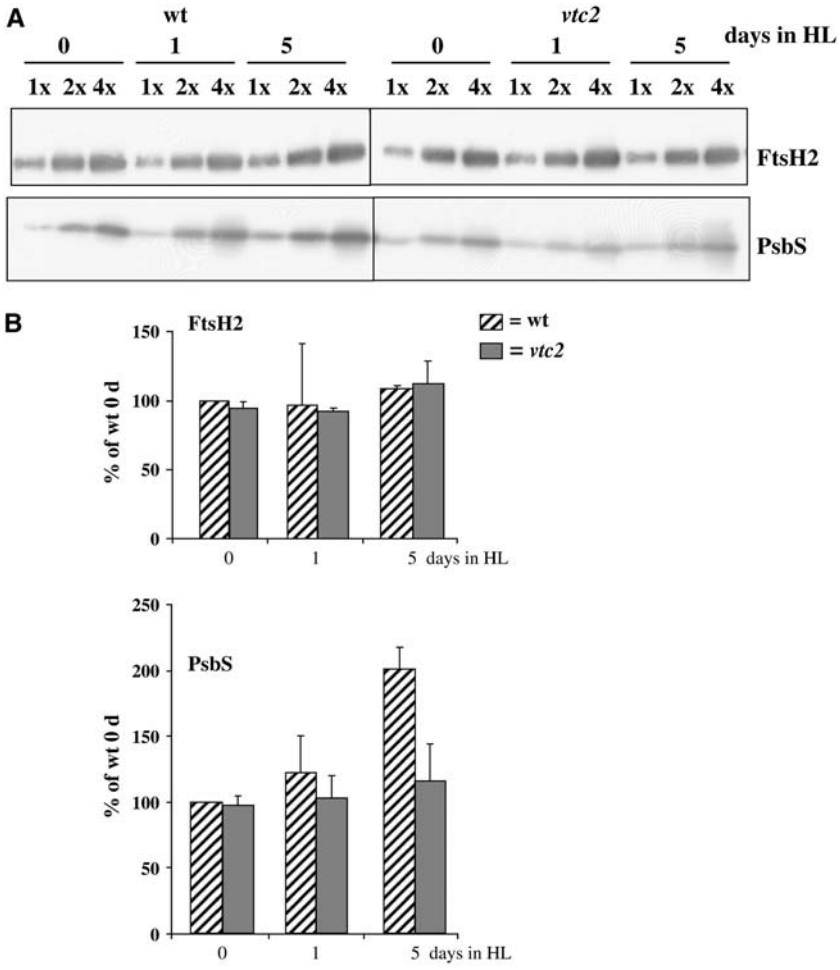

Figure 6. Response of integral thylakoid membrane proteins FtsH2 and PsbS to 0, 1, and 5 d HL treatment in wild type and *vtc2*. Western-blot analysis (A) and its quantification (B) of FtsH2 and PsbS. A total of 10, 20, and 40 μg of total leaf membrane proteins were loaded per gel lane (indicated as 1x, 2x, and 4x). The experiment was repeated twice with independent biological replicates (n = 2). The bar diagrams show the quantification for both FtsH2 and PsbS with SDS.

independent biological replicates and thus involved 72 gels, 5) spots were stained with the fluorescent dye Sypro Ruby for better linearity and matched with image analysis software, followed by a very extensive manual spot matching verification, 6) a multivariance analysis was carried out with a conservative data set, omitting spots that could not be detected in each of the genotype-treatment combinations, and 7) the four time points (rather than one or two) used in this study helped to assess the consistency of the protein response. In total, 155 consistent and quantified spots were observed in all treatment-genotype combinations, and were statistically tested for significance.

To understand the protein population that was actually sampled in the experiments, we tried to identify all protein spots detected on the gels using nanoLC-ESI tandem MS. All MS data were searched against the latest annotation of the Arabidopsis genome (v6), released by The Arabidopsis Information Resource in December, 2005 (http://www.arabidopsis.org/); 99 proteins were identified in various functional categories, with only three nonchloroplast proteins. This included 25 confirmed lumenal proteins, 11 PG proteins, and five thioredoxins/peroxiredoxins. Many of those were identified in earlier thylakoid proteome studies (Peltier et al., 2002; Schubert et al., 2002; Friso et al., 2004; Peltier et al., 2004) or in the thylakoid-associated PGs (Vidi et al., 2006; Ytterberg et al., 2006). As an added feature, we also extracted the peptide sequences that were used for identification and made those available via the Plastid Proteome Database (http://ppdb.tc.cornell.edu/). The peptide sequences are projected on the annotated protein sequences, and with the reported MOWSE scores, provide a clear summary of the protein identification. A summary with the most significant proteins is shown in Figure 7.

Up-Regulation of Plastoglobular Proteins in Response to HL Treatment

Seven proteins in the soluble thylakoid proteome were consistently 2- to 10-fold up-regulated in response to the transition to HL in both genotypes. These were four members of the FIBs family (Fib1a, 1b, 2, and 7), Fru-biphosphate aldolase-1, a flavin reductase-related protein, and YCF37. Importantly, except for YCF37, these proteins were just recently shown to be part of thylakoid-associated PGs (Vidi et al., 2006; Ytterberg et al., 2006). These studies suggest that PGs in chloroplasts are a site of synthesis and accumulation

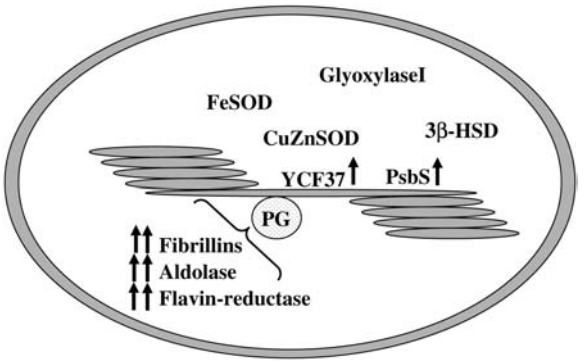

Figure 7. Summary of identified proteins that respond most significantly to the HL treatment and/or the ascorbate deficiency. Arrows mark proteins that are strongly (several fold) up-regulated in response to the transition to HL. 3β-HSD, 3-β-hydroxysteroid-dehydrogenase.

of vitamin E and quinones and also likely play a role in breakdown of carotenoids and turnover of lipids/fatty acids. Since the PG proteome is a subfraction of the peripheral thylakoid proteome, it is not surprising that we identified and quantified in this study only the most abundant proteins in PGs. Since most of the PG-localized proteins appeared to be coregulated under extreme and prolonged light stress (7 d upon continued HL; Ytterberg et al., 2006), accumulation levels of most of the other PG-associated proteins, which are of much lower abundance, are probably also increased under the HL conditions in this study.

Up-Regulation of a Thylakoid Tetratricopeptide Repeat Protein with a Putative PSI Assembly Function

YCF37 was 2-fold up-regulated after 5 d of HL in both wild type and *vtc2*. YCF37 is a protein with a tetratricopeptide repeat and is a homolog of a thylakoid-associated protein in the cyanobacterium *Synechocystis* sp. PCC 6803. In cyanobacteria it was shown to be a thylakoid protein involved in PSI assembly or oligomerization (Wilde et al., 2001; Dühring et al., 2006). YCF37 has not been observed before in chloroplasts. Although light-induced damage of the thylakoid is best known for PSII, PSI can also be inactivated and damaged during light stress. In Arabidopsis, it appears that the light-harvesting complex I antennae can be recycled to some extent upon damage to PSI, while the PSI core complex turns over in its entirety (Zhang and Scheller, 2004; Scheller and Haldrup, 2005). We speculate that the HL-induced increase of YCF37 relates to possible accelerated turnover and repair of PSI.

Several Proteases and Other Thylakoid-Associated Proteins Do Not Significantly Respond to HL Stress and Ascorbate Deficiency

The lumenal proteases DegP2,5 and thylakoid FtsH2 (VAR2) were not affected by light treatment or by low ascorbate concentration in *vtc2*. In contrast, the Ser type IV thylakoid protease SPPA was strongly up-regulated in response to the HL transition (data not shown), as was also earlier demonstrated (Lensch et al., 2001). With the exception of FtsH8, the overall FtsH protein levels do not substantially respond to stress conditions (Sinvany-Villalobo et al., 2004; Sakamoto, 2006). Nevertheless, a notable role of FtsH in chloroplasts is its involvement in the PSII repair cycle. Chlorophyll fluorescence induction analysis in green sectors of *var1* and *var2* showed that these mutants greatly reduced PSII activity when irradiated under HL (Bailey et al., 2002; Sakamoto et al., 2002; Sakamoto et al., 2003). In fact, HL-dependent degradation of D1 did occur in wild-type leaves, but not in *var2* leaves (Chen et al., 2000; Bailey et al., 2002). Other lumenal- and thylakoid-associated proteins that were quantified, but that did not show a response to ascorbate or light stress, include two lumenal protein isomerases and Prx A and E.

Differential Response between *vtc2* and Wild Type; Does the Ascorbate Concentration Matter?

Differential accumulation of a number of proteins was observed between wild type and *vtc2*. These included Fe-SODs and Cu,Zn-SOD, HSP70, PsbS, and a chloroplast-localized glyoxalate I, all of which have been associated with stress-response functions. The differential accumulation of these proteins shows that the ascorbate deficiency does have a significant, albeit small impact on the chloroplast stress response. We observed significant increase of cpHSP70-1 and cpHSP70-2 in *vtc2*, but not in wild type, after 3 and 5 d of HL. The two HSP70 homologs are predominantly present in the chloroplast stroma, but can associate to the thylakoid membrane. It was suggested that HSP70 in *Chlamydomonas reinhardtii* chloroplasts may participate in molecular protection of the PSII reaction centers during photoinhibition and in the process of PSII repair (Schroda et al., 1999). Lactoylglutathionelyase or glyoxalase I participates in the glutathione-dependent cellular detoxification of cytotoxic methylglyoxal, but its precise role in the plastid remains unclear.

PsbS is a component of PSII and has been shown to play a key role in protection of PSII through release of excess excitation energy, observed as rapidly inducible nonphotochemical quenching (Li et al., 2000). PsbS levels were similar in wild type and *vtc2*, but upon the HL treatment PsbS was up-regulated 2-fold in wild type but not in *vtc2*. *vtc2* was shown to have reduced levels of nonphotochemical quenching because violaxanthin deepoxidase in the lumen requires ascorbate as cofactor for violaxanthin to zeaxathin conversion (Müller-Moulé et al., 2002).

CONCLUSION

The chloroplast has a tremendous capacity to respond to changes in light regime through a wide

variety of mechanisms operating at different time scales from seconds to days. Moreover, the multilayered ROS detoxification system, involving, for example, carotenoids, ascorbate, tocopherol, glutathione, and the thioredoxins/peroxiredoxins, shows very effective compensation mechanisms for the absence or weakening of one of the detoxification systems. Thus the proteome of chloroplasts forms an effective stress defense network, with the PG proteome likely playing an important role. Future efforts to understand the multilayered chloroplast stress-response network must include the enzymatic role of this enigmatic lipid-rich compartment.

MATERIALS AND METHODS

Plant Material, Growth Conditions, and HL Treatment

Arabidopsis (*Arabidopsis thaliana*) wild type (ecotype Columbia-0) and *vtc2-2* were grown on soil in growth chambers (Conviron) under controlled conditions (70% relative humidity, 120 μmol photons m^{-2} s^{-1}, 10 h photoperiod, and 22°C light/17°C dark). The *vtc2-2* line was originally identified as described in Conklin et al. (2000) and subsequent map-based cloning showed that the line has a missense mutation in At4g26850, leading to a Gly-to-Asp change in predicted exon 5 (Jander et al., 2002). The *vtc2-2* seeds were kindly provided by Dr. P. Conklin (in 2003). Approximately 40 d after sowing when plants had fully developed leaf rosettes, but were prior to bolting, the light intensity was increased to 1,000 μmol photons m^{-2} s^{-1} (HL) while maintaining the light-dark cycle. Complete rosettes were harvested after 0, 1, 3, and 5 d of the HL treatment. All plant material was collected after 2 h into the light period.

Chlorophyll Fluorescence Measurements

F_v/F_m values (as a measure of PSII intactness) of attached leaves were determined during the first half of the light period after a 15 min dark adaptation period, using a pulse modulated fluorimeter (HansaTech, FMS2).

Ascorbate and Anthocyanin Determinations

For determination of ascorbate, 0.4 mg leaf tissue was ground in liquid nitrogen and suspended in 2% meta-phosphoric acid and 2 mM EDTA. Membranes were removed by centrifugation at 18,000*g* for 10 min at 4°C. The soluble extract was neutralized with sodium phosphate buffer (pH 6.8) to a final concentration of 0.1 M. Ascorbate and dehydro ascorbate were measured according to Casper-Lindley and Björkman (1996). Anthocyanins were extracted from 0.2 g of leaf tissue ground in liquid nitrogen, by addition of 1 mL water, and centrifugation at 18,000*g* for 10 min. The supernatant was diluted with 0.4 M sodium acetate at pH 4.5 and 25 mM potassium chloride at pH 1.0, and then spun again. Total monomeric anthocyanins were measured by recording the A_{520} as outlined in Giusti and Wrolstad (2001).

Protein Purification and Determination, 2DE Analysis and Staining

Intact thylakoid membranes were purified on Percoll gradients essentially as in Friso et al. (2004). The soluble thylakoid proteome (lumen and peripherally attached proteins) were released by mild sonication (three times for 20 s at 10 W) with a Fisher Scientific membrane dismembrator (model 100) from a 3 mL thylakoid suspension at 1 mg chlorophyll mL^{-1}. Soluble proteins were separated from the membrane fraction by centrifugation at 55,000*g* for 25 min at 4°C, and then precipitated in 80% acetone. The protein pellet was suspended in 9 M urea, 4% CHAPS, 0.5% Triton X-100, and 0.5% glycerol. Protein concentrations were determined with the Bradford method (Bradford, 1976). For isoelectric focusing, 2% IPG buffer pH 4 to 7 (Amersham) and 2 mM tri-butylphosphine were added to the protein samples. One-hundred micrograms of proteins were loaded on IPG strips pI 4 to 7 (11 cm; Pharmacia). Focusing, followed by reduction and alkylation were carried out as described earlier (Peltier et al., 2000). Precast Tris-HCl gels (8%–16% acrylamide; Bio-Rad) were used in the second dimension. Gels were stained for 12 h with Sypro Ruby (Molecular Probes).

Image Analysis

Gel images were taken with a Fluor-S imager (Bio-Rad) using several exposure times, ranging from 3 to 50 s. These images were evaluated for signal-to-noise ratio, sensitivity (number of detected spots), and number of saturated spots. Images with relatively low exposure times were chosen for analysis since they had the best signal-to-noise ratio (estimated as spot intensity over background), while allowing detection of low abundant spots (data not shown). The chosen gel images had maximally from five to nine saturated spots in particular containing plastocyanin, OEC23, OEC33, and $CF_1\alpha$. Spot 955 ($CF1\alpha$) and spot 386 (plastocyanin) were the most frequently saturated (on 27 and 28 gels over 72). Image analysis was carried out using HT analyzer 2.1 (Genomic Solutions). Gels with extensive streaking or poor spot resolution were discarded and new gels were run with the same sample. In total, 72 gel images were used for the final data set (two genotypes [wild type and *vtc2*], four time points [0, 1, 3, and 5 d of HL], three gels for each sample, and three independent experiments). Spot detection was performed using the same settings for all the gel images. To clean the images from false spots (e.g. Sypro Ruby deposits, water bubbles, etc.), each gel was visually inspected and fictitious spots manually removed in HT analyzer. After background subtraction the spot intensity was normalized as percentage of the total spot intensity of the gel. One gel was chosen as a reference and corresponding spots on the 72 gels were matched to the reference gel.

Statistical Analysis

To minimize the contribution of gel-to-gel variation, three gels were run for each sample. The logarithm of intensity of correspondent spots on the three gels were averaged and considered as data points. The intensities of non-detected spots were treated as missing values rather than zeros, and did not contribute to the average intensity.

A multivariance model was used to evaluate plant effect (due to wild-type and *vtc2* genotypic backgrounds), treatment effect (due to the light stress observed at the four time points), and genotype-treatment interaction. The statistical model was applied to 155 spots with complete data. We then tested the effect of the HL treatment and the genotype, as well as their interaction using the following equation: variation = (genotype) + (treatment) + (genotype-treatment) + (residual error). The significance was measured by both the *P* value and the false-positive discovery rate, calculated as identified significant spots divided by expected number of false-positive spots. A randomization argument was used to adjust the obtained *P* values, according to the formula: p_adj = (rank of unadjusted p among 155 pseudo *P* value)/156. We will discuss two groups of spots that show differences with a probability *P* of error less than 0.01 and less than 0.05.

MS

Protein spots were excised from the gels and automatically (Progest, Genomic Solutions) or manually digested with trypsin or chymotrypsin. After digestion, peptides were analyzed using a CapLC-ESI-MS/MS (Q-TOF1; Waters). Peptides were loaded on a μguard column (LC-packings; MGU-30-C18PM), followed by separation on a PepMap C18 Reverse Phase Nano column (LC Packings nan75-15–03-C18PM), using 45 min gradients with 95% water, 5% acetonitrile, 0.1% formic acid (solvent A), and 95% acetonitrile, 5% water, 0.1% formic acid (solvent B), and a flow rate of 0.2 μL/min. MS/MS spectra were processed using Mascot distiller (v2.1) and the proteins were identified by searching against the Arabidopsis database, ATH1.pep (v6.0), using in-house Mascot (Matrix Science). Mascot search criteria were as follows: maximal precursor ion and fragment ion errors 1.2 and 0.8 D, variable Met oxidation, maximally 1 missed cleavage, minimal significance for protein MOWSE score $P < 0.01$, and minimal ion score 20. These search results were further filtered (using an in-house routine; Q. Sun and K.J. van Wijk, unpublished data), to remove all protein identifications that needed peptides matched at rank 2 or higher to realize a significant MOWSE score (at $P < 0.01$). To ensure correct assignment of protein identity to weaker selected spots (intensity <0.2% of the total volume), differentially expressed spots were identified from two or more gels, and additional verification of spot matching. In a few cases we identified more than one protein in a particular spot (as indicated). Where possible, the protein with a significantly larger number of

matching peptides and higher MOWSE score was assigned as the major contributor to the spot intensity. Identified proteins with MOWSE scores and matched peptide sequences can be found in the Plastid Proteome Database at http://ppdb.tc.cornell.edu.

Western-Blot Analysis

For analysis of cellular proteins by western blots, wild type and *vtc2* leaves were extracted by mortar and pestle in liquid nitrogen and 10 mM Tris-HCL buffer pH 6.8, and 2 mM EDTA. The extracts were spun at 18,000*g* for 10 min at 4°C, the supernatant was transferred to a new tube, and spun at 55 k rpm in TLA100.3. The resulting clear supernatant contained the total soluble proteins, which were precipitated in 10% TCA for 30 min on ice. The pellets were washed with Tris and resuspended in 2× Laemmli buffer (125 mM Tris pH 6.8, 4% SDS, and 10% glycerol). The pellet from the 55 k spin was washed with tris-EDTA, spun again, and then resuspended in 2× Laemmli buffer. Following solubilization, insoluble material was removed by a 5 min centrifugation at 18,000*g* and the supernatant was reduced and used for SDS-PAGE analysis on 12% acrylamide gels. Proteins were blotted on polyvinylidene difluoride membrane, incubated overnight with primary antisera (1:1,000–1:5,000) directly against Arabidopsis proteins (anti-Fe-SOD, anti-Cu,Zn-SOD, anti-FtsH2, and anti-PsbS), and a potato (*Solanum tuberosum*) anti-CDSP34 (Langenkämper et al., 2001) and then detected with a horseradish (*Armoracia lapathifolia*) peroxidase-conjugated secondary antibody (Sigma) and enhanced chemiluminescence. Anti-Fe-SOD, anti-Cu,Zn-SOD, anti-FtsH2, anti-PsbS, and anti-CDSP34 were provided by P. Conklin, W. Sakamoto, K.K. Niyogi, and P. Rey, respectively.

ACKNOWLEDGMENTS

We thank Professor J. Booth at the Department of Statistics for his excellent help with the statistical analysis. We thank Dr. Patricia Conklin for donation of the *vtc2-2* mutant seeds and for the SODs antibodies, Dr. Antonio Masi for help with the ascorbate determinations and discussions, Dr. P. Rey for the CDSP34 antibody, Dr. W. Sakamoto for antisera against FtsH2,5, Dr. K.K. Niyogi for anti-PsbS, and Dr. K.J. Dietz for anti-2-Cys Prx. We thank Dr. W. Majeran and H. Rutschow for comments and discussion.

Received March 14, 2006; revised April 19, 2006; accepted April 21, 2006; published April 28, 2006.

LITERATURE CITED

Abdel-Ghany SE, Müller-Moulé P, Niyogi KK, Pilon M, Shikanai T (2005) Two P-type ATPases are required for copper delivery in *Arabidopsis thaliana* chloroplasts. Plant Cell **17:** 1233–1251

Apel K, Hirt H (2004) Reactive oxygen species: metabolism, oxidative stress, and signal transduction. Annu Rev Plant Biol **55:** 373–399

Bailey S, Thompson E, Nixon PJ, Horton P, Mullineaux CW, Robinson C, Mann NH (2002) A critical role for the Var2 FtsH homologue of Arabidopsis thaliana in the photosystem II repair cycle in vivo. J Biol Chem **277:** 2006–2011

Bassi R, Caffarri S (2000) Lhc proteins and the regulation of photosynthetic light harvesting function by xanthophylls. Photosynth Res **64:** 243–256

Bradford MM (1976) A rapid sensitive method for the quantification of microgram quantities of protein utilizing the principle of protein-dye binding. Anal Biochem **72:** 248–254

Buchanan BB, Balmer Y (2005) Redox regulation: a broadening horizon. Annu Rev Plant Biol **56:** 187–220

Casper-Lindley C, Björkman O (1996) Nigericin insensitive post-illumination reduction in fluorescence yield in Dunaliella tertiolecta (chlorophyte). Photosynth Res **50:** 209–222

Chen M, Choi Y, Voytas DF, Rodermel S (2000) Mutations in the Arabidopsis VAR2 locus cause leaf variegation due to the loss of a chloroplast FtsH protease. Plant J **22:** 303–313

Conklin PL, Saracco SA, Norris SR, Last RL (2000) Identification of ascorbic acid-deficient Arabidopsis thaliana mutants. Genetics **154:** 847–856

Davletova S, Rizhsky L, Liang H, Shengqiang Z, Oliver DJ, Coutu J, Shulaev V, Schlauch K, Mittler R (2005) Cytosolic ascorbate peroxidase 1 is a central component of the reactive oxygen gene network of Arabidopsis. Plant Cell **17:** 268–281

Dietz KJ, Scheibe R (2004) Redox regulation: an introduction. Physiol Plant **120:** 1–3

Dühring U, Irrgang KD, Lunser K, Kehr J, Wilde A (2006) Analysis of photosynthetic complexes from a cyanobacterial ycf37 mutant. Biochim Biophys Acta **1757:** 3–11

Foyer CH, Noctor G (2005) Redox homeostasis and antioxidant signaling: a metabolic interface between stress perception and physiological responses. Plant Cell **17:** 1866–1875

Friso G, Giacomelli L, Ytterberg AJ, Peltier JB, Rudella A, Sun Q, Wijk KJ (2004) In-depth analysis of the thylakoid membrane proteome of *Arabidopsis thaliana* chloroplasts: new proteins, new functions, and a plastid proteome database. Plant Cell **16:** 478–499

Gillet B, Beyly A, Peltier G, Rey P (1998) Molecular characterization of CDSP 34, a chloroplastic protein induced by water deficit in Solanum tuberosum L. plants, and regulation of CDSP 34 expression by ABA and high illumination. Plant J **16:** 257–262

Giusti MM, Wrolstad RE (2001) Characterization and Measurement of Anthocyanins by UV-Visible Spectroscopy. *In* RE Wrolstad, TE Acree, EA Decker, MH Penner, DS Reid, SJ Schwartz, CF Shoemaker, D Smith, P Sporns, eds, Current Protocols in Food Analytical Chemistry. John Wiley & Sons, New York

Gómez SM, Nishio JN, Faull KF, Whitelegge JP (2002) The chloroplast grana proteome defined by intact mass measurements from liquid chromatography mass spectrometry. Mol Cell Proteomics **1:** 46–59

Holt NE, Fleming GR, Niyogi KK (2004) Toward an understanding of the mechanism of nonphotochemical quenching in green plants. Biochemistry **43:** 8281–8289

Jander G, Norris SR, Rounsley SD, Bush DF, Levin IM, Last RL (2002) Arabidopsis map-based cloning in the post-genome era. Plant Physiol **129:** 440–450

Kessler F, Schnell D, Blobel G (1999) Identification of proteins associated with plastoglobules isolated from pea (Pisum sativum L.) chloroplasts. Planta **208:** 107–113

Kiddle G, Pastori GM, Bernard S, Pignocchi C, Antoniw J, Verrier PJ, Foyer CH (2003) Effects of leaf ascorbate content on defense and photosynthesis gene expression in Arabidopsis thaliana. Antioxid Redox Signal **5:** 23–32

Langenkämper G, Manac'h N, Broin M, Cuiné S, Becuwe N, Kuntz M, Rey P (2001) Accumulation of plastid lipid-associated proteins (fibrillin/CDSP34) upon oxidative stress, ageing and biotic stress in Solanaceae and in response to drought in other species. J Exp Bot **52:** 1545–1554

Lensch M, Herrmann RG, Sokolenko A (2001) Identification and characterization of SppA, a novel light-inducible chloroplast protease complex associated with thylakoid membranes. J Biol Chem **276:** 33645–33651

Li XP, Björkman O, Shih C, Grossman AR, Rosenquist M, Jansson S, Niyogi KK (2000) A pigment-binding protein essential for regulation of photosynthetic light harvesting. Nature **403:** 391–395

Mahalingam R, Shah N, Scrymgeour A, Fedoroff N (2005) Temporal evolution of the Arabidopsis oxidative stress response. Plant Mol Biol **57:** 709–730

Mittler R, Vanderauwera S, Gollery M, Van Breusegem F (2004) Reactive oxygen gene network of plants. Trends Plant Sci **9:** 490–498

Monte E, Ludevid D, Prat S (1999) Leaf C40.4: a carotenoid-associated protein involved in the modulation of photosynthetic efficiency? Plant J **19:** 399–410

Müller-Moulé P, Conklin PL, Niyogi KK (2002) Ascorbate deficiency can limit violaxanthin de-epoxidase activity in vivo. Plant Physiol **128:** 970–977

Müller-Moulé P, Golan T, Niyogi KK (2004) Ascorbate-deficient mutants of Arabidopsis grow in high light despite chronic photooxidative stress. Plant Physiol **134:** 1163–1172

Müller-Moulé P, Havaux M, Niyogi KK (2003) Zeaxanthin deficiency enhances the high light sensitivity of an ascorbate-deficient mutant of Arabidopsis. Plant Physiol **133:** 748–760

Mullineaux P, Karpinski S (2002) Signal transduction in response to excess light: getting out of the chloroplast. Curr Opin Plant Biol **5:** 43–48

Nagata T, Todoriki S, Masumizu T, Suda I, Furuta S, Du Z, Kikuchi S (2003) Levels of active oxygen species are controlled by ascorbic acid and anthocyanin in Arabidopsis. J Agric Food Chem **51:** 2992–2999

Niyogi KK (2000) Safety valves for photosynthesis. Curr Opin Plant Biol **3:** 455–460

Pastori GM, Foyer CH (2002) Common components, networks, and pathways of cross-tolerance to stress: the central role of ''redox'' and abscisic acid-mediated controls. Plant Physiol **129:** 460–468

Pastori GM, Kiddle G, Antoniw J, Bernard S, Veljovic-Jovanovic S, Verrier PJ, Noctor G, Foyer CH (2003) Leaf vitamin C contents modulate plant defense transcripts and regulate genes that control development through hormone signaling. Plant Cell **15:** 939–951

Peltier JB, Emanuelsson O, Kalume DE, Ytterberg J, Friso G, Rudella A, Liberles DA, Soderberg L, Roepstorff P, von Heijne G, et al (2002) Central functions of the lumenal and peripheral thylakoid proteome of Arabidopsis determined by experimentation and genome-wide prediction. Plant Cell **14:** 211–236

Peltier JB, Friso G, Kalume DE, Roepstorff P, Nilsson F, Adamska I, van Wijk KJ (2000) Proteomics of the chloroplast: systematic identification and targeting analysis of lumenal and peripheral thylakoid proteins. Plant Cell **12:** 319–342

Peltier JB, Ytterberg AJ, Sun Q, van Wijk KJ (2004) New functions of the thylakoid membrane proteome of Arabidopsis thaliana revealed by a simple, fast, and versatile fractionation strategy. J Biol Chem **279:** 49367–49383

Rey P, Gillet B, Romer S, Eymery F, Massimino J, Peltier G, Kuntz M (2000) Over-expression of a pepper plastid lipid-associated protein in tobacco leads to changes in plastid ultrastructure and plant development upon stress. Plant J **21:** 483–494

Rossel JB, Wilson IW, Pogson BJ (2002) Global changes in gene expression in response to high light in Arabidopsis. Plant Physiol **130:** 1109–1120

Sakamoto W (2006) Protein degradation machineries in plastids. Annu Rev Plant Biol **57:** 599–621

Sakamoto W, Tamura T, Hanba-Tomita Y, Murata M (2002) The VAR1 locus of Arabidopsis encodes a chloroplastic FtsH and is responsible for leaf variegation in the mutant alleles. Genes Cells **7:** 769–780

Sakamoto W, Zaltsman A, Adam Z, Takahashi Y (2003) Coordinated regulation and complex formation of yellow variegated1 and yellow variegated2, chloroplastic FtsH metalloproteases involved in the repair cycle of photosystem II in Arabidopsis thylakoid membranes. Plant Cell **15:** 2843–2855

Scheller HV, Haldrup A (2005) Photoinhibition of photosystem I. Planta **221:** 5–8

Schroda M, Vallon O, Wollman FA, Beck CF (1999) A chloroplast-targeted heat shock protein 70 (HSP70) contributes to the photoprotection and repair of photosystem II during and after photoinhibition. Plant Cell **11:** 1165–1178

Schubert M, Petersson UA, Haas BJ, Funk C, Schröder WP, Kieselbach T (2002) Proteome map of the chloroplast lumen of Arabidopsis thaliana. J Biol Chem **277:** 8354–8365

Shürmann P, Jacquot J-P (2000) Plant thioredoxin systems revisited. Annu Rev Plant Physiol Plant Mol Biol **51:** 371–400

Sinvany-Villalobo G, Davydov O, Ben-Ari G, Zaltsman A, Raskind A, Adam Z (2004) Expression in multigene families: analysis of chloroplast and mitochondrial proteases. Plant Physiol **135:** 1336–1345

Takahama U, Oniki T (1992) Regulation of peroxidase-dependent oxidation of phenolics in the apoplast of spinach leaves by ascorbate. Plant Cell Physiol **33:** 379–387

van Wijk KJ (2004) Plastid proteomics. Plant Physiol Biochem **42:** 963–977

Vanderauwera S, Zimmermann P, Rombauts S, Vandenabeele S, Langebartels C, Gruissem W, Inze D, Van Breusegem F (2005) Genome-wide analysis of hydrogen peroxide-regulated gene expression in Arabidopsis reveals a high light-induced transcriptional cluster involved in anthocyanin biosynthesis. Plant Physiol **139:** 806–821

Veljovic-Jovanovic SD, Pignocchi C, Noctor G, Foyer CH (2001) Low ascorbic acid in the vtc-1 mutant of Arabidopsis is associated with decreased growth and intracellular redistribution of the antioxidant system. Plant Physiol **127:** 426–435

Vidi PA, Kanwischer M, Baginsky S, Austin JR, Csucs G, Dörmann P, Kessler F, Bréhélin C (2006) Tocopherol cyclase (VTE1) localization and vitamin E accumulation in chloroplast plastoglobule lipoprotein particles. J Biol Chem **281:** 11225–11234

Wilde A, Lünser K, Ossenbühl F, Nickelsen J, Börner T (2001) Characterization of the cyanobacterial ycf37: mutation decreases the photosystem I content. Biochem J **357:** 211–216

Wilmouth RC, Turnbull JJ, Welford RW, Clifton IJ, Prescott AG, Schofield CJ (2002) Structure and mechanism of anthocyanidin synthase from Arabidopsis thaliana. Structure **10:** 93–103

Ytterberg AJ, Peltier JB, van Wijk KJ (2006) Protein profiling of plastoglobules in chloroplasts and chromoplasts: a surprising site for differential accumulation of metabolic enzymes. Plant Physiol **140:** 984–997

Zhang S, Scheller HV (2004) Photoinhibition of photosystem I at chilling temperature and subsequent recovery in Arabidopsis thaliana. Plant Cell Physiol **45:** 1595–1602